

Chapter 3

**PDMS IN URINARY TRACT DEVICES:
APPLICATIONS, PROBLEMS
AND POTENTIAL SOLUTIONS**

***M. Gomes, L. C. Gomes, R. Teixeira-Santos
and F. J. Mergulhão****

LEPABE - Laboratory for Process Engineering, Environment,
Biotechnology and Energy, Faculty of Engineering, University of Porto,
Rua Dr. Roberto Frias, Portugal

ABSTRACT

PDMS is one of the most widely used polymers for the fabrication of biomedical devices. Of particular relevance is the application of PDMS in urinary tract devices such as urinary catheters and ureteral stents. As these devices are being used by a growing number of patients and indwelling times are increasing in an aging population, the incidence of urinary tract infections is rising. These infections have implications on the quality of life of the patients and represent a severe burden on healthcare systems.

* Corresponding Author's E-mail: filipem@fe.up.pt.

This chapter reviews the main uses of PDMS in urinary tract devices and associated complications. As new solutions are needed to reduce bacterial adhesion and biofilm formation on PDMS-based devices, a testing platform is described to evaluate surface performance in both urinary catheters and ureteral stents. Examples of these solutions are also discussed in a quest for more efficient urinary tract devices.

Keywords: PDMS-based surfaces, urinary catheters, ureteral stents, urinary tract infections, antibiofilm coatings, flow systems

ABBREVIATIONS

3D	three-dimensional
AgNP	silver nanoparticles
AMP	antimicrobial peptide
CAUTI	catheter-associated urinary tract infection
CFD	computational fluid dynamics
CFU	colony forming unit
CLSM	confocal laser scanning microscopy
DAPI	4'-6-diamidino-2-phenylindole
ECDC	European Centre for Disease Prevention and Control
EPS	extracellular polymeric substance
FDA	Food and Drug Administration
GA	gallic acid
HAI	healthcare-associated infection
IAR	initial adhesion rate
L-AmB	liposomal amphotericin B
MRD	modified Robbins device
MRSA	methicillin-resistant <i>Staphylococcus aureus</i>
PC	phosphoryl-choline
PCA	plate count agar
PDA	polydopamine
PEG	polyethylene glycol

PLC(P)	polycaprolactone polymer
PPFC	parallel plate flow chamber
PTFE	polytetrafluoroethylene
SD	standard deviation
SMZ	sulfamethoxazole
TANP	tetraetherlipid-silver nanoparticle-norfloracin-poly lactide
TMP	trimethoprim
UTD	urinary tract device
UTI	urinary tract infection
UV	ultraviolet
VRE	vancomycin-resistant enterococci

1. INTRODUCTION

Since the 1960s, silicone materials have been extensively applied in the medical field due to their high biocompatibility [1, 2]. Polydimethylsiloxane (PDMS) is one of the most used class of commercially available silicone polymers [3, 4]. This polymer is non-toxic, biological and chemically inert, optically clear, elastomeric, gas-permeable, hydrophobic, mechanically resistant, and inexpensive [4, 5]. Moreover, the risk of PDMS biodegradation and migration appears to be inexistent [6]. Therefore, the high biocompatibility and stability of PDMS contributed to its success in several medical applications, including the development of urinary tract devices (UTDs) [4, 7].

The several benefits of silicone compared to other available biomaterials have made it the material of choice for the construction of urinary tract devices [8]. However, despite of its outstanding properties, silicone is prone to bacterial adhesion and biofilm formation [9, 10]. The complications associated with the use of indwelling urinary catheters and ureteral stents have driven the technological evolution in the surface coatings. Up to date, numerous studies have described different coating

strategies changing the PDMS physicochemical properties or conferring it antimicrobial potential.

In this chapter, the PDMS-based surfaces developed to prevent urinary tract infections (UTIs) will be reviewed. Additionally, different flow systems available for surface evaluation will be discussed and their importance will be evidenced with an experimental approach to study bacterial adhesion and biofilm formation under hydrodynamic conditions that mimic those found in urinary catheters and ureteral stents.

2. PDMS IN URINARY TRACT DEVICES

Urinary tract devices, including urinary catheters and ureteral stents, are some of the most widely used medical devices in hospitals and healthcare facilities. The first urinary devices were constructed using metallic materials such as copper, tin, bronze and gold [9]. However, in the last decades, metals were replaced by polyvinylchloride, polyurethanes, silicone and latex rubbers in order to reduce their rigidity [8-10]. Over the years, polymeric materials have been improved towards higher biocompatibility, tensile strength, softness and elasticity, and biological and chemical resistance [9, 11, 12]. Table 1 lists the advantages and disadvantages of different biomaterials used in the manufacture of UTDs.

Silicone presents several advantages compared to other polymeric materials. Due to the nontoxic and inert nature of silicone, this polymer displays higher tissue compatibility than latex or polyvinylchloride. Simultaneously, it is non-irritating and non-sensitizing, having low surface tension and moderate resistance to abrasion and external compression. Conversely to latex, silicone is UV and chemical resistant and is more thermally stable than polyurethane. However, although this biomaterial reveals desirable properties for a urinary device, silicone has a low drainage efficacy. In terms of encrustation, there is a reduced incidence of struvite and calcium phosphate hydroxyapatite stones, whereas encrustation by calcium carbonate and calcium oxalate stones is more frequent. Moreover, similarly to latex and polyurethane, silicone is prone

to bacterial adhesion [8-10]. Despite having some disadvantages, silicone has become the “gold standard” material for urinary devices [9-12].

**Table 1. Biomaterials used for urinary tract devices:
Advantages and disadvantages**

Material	Advantages	Disadvantages
Silicone	Biocompatible Non-irritating and non-sensitizing Chemically and thermally stable UV resistant Low surface tension Moderate resistance to abrasion Improves surface lubrication Long lifetime before encrustation and blockage Highly resistant to external compression Decreased struvite and calcium phosphate stones incidence Inexpensive	Can be uncomfortable due to its rigidity Prone to premature device failure Prone to bacterial adhesion Decreased drainage efficacy Prone to encrustation by calcium carbonate and calcium oxalate stones
Latex	Can be modified by hydrogel or Teflon coatings Inexpensive Easily manipulated High tensile strength	Poor biocompatibility Poor UV and chemical resistance Poor tissue adherence Can promote biofilm formation and encrustation Causes allergic reactions
Polyurethane	Excellent biocompatibility Soft and smooth Resistant to external forces	Sensitivity to heat Cannot be autoclaved Prone to bacterial adhesion Prone to encrustation by calcium carbonate and calcium oxalate stones
Polyvinyl-chloride	Long lifetime Chemically stable Inexpensive	Reduced flexibility Public health concerns due to additives that can leach <i>in vivo</i>

Compiled using data from [8-11].

Based on these evidences, several authors have studied the efficacy of PDMS urinary catheters on the prevention of catheter-associated infections. Moola and Konno conducted a systematic review about the management of indwelling urethral catheters to prevent UTIs where uncoated silicone catheters were compared with other types of catheters

[13]. According to this study, there were no differences between PDMS and latex urethral catheters. However, the use of PDMS catheters was associated with an overall infection rate of 2.1% at 24 h, 6.8% at 48 h, and 20% at 96 h [13]. Stenzenlius et al. reported similar results for PDMS urinary catheters (an incidence of bacteriuria of 5.5%) after a mean period of 2 days of catheterization [14]. Additionally, Thibon and co-workers demonstrated that silicone Foley catheters had a cumulative bacteriuria incidence of 11.9% [15]. Lastly, Moola and Konno also registered an incidence of bacteriuria and funguria per 1000 catheter days of 38.6% for silicon catheters [13].

Regarding PDMS ureteral stents, there are few data demonstrating their efficacy. According to Hoe, although silicone stents are tolerated by patients and associated with low complication rates, 28% of inserted stents failed [16]. Conversely, a study carried out by Tunney et al. demonstrated that silicone has a higher resistance to encrustation compared to other materials [17].

Thus, the complications associated with silicone urinary tract devices warn of the need to develop new PDMS-based surfaces to avoid bacterial colonization and encrustation.

3. PROBLEMS ASSOCIATED TO URINARY TRACT DEVICES

Urinary tract devices have been widely applied in the treatment and mitigation of some diseases, improving the quality of life of the patients. However, despite all care and preventive measures taken to avoid contamination during the insertion of these devices, UTIs are increasingly common.

UTIs are one of the most common healthcare-associated infections (HAIs), being responsible for about 17% of hospital-acquired bacteremia [18]. In fact, the HAI annual incidence reports pointed to a prevalence of 36% and 27% of hospital-wide UTIs in the United States and Europe, respectively [19, 20]. Furthermore, the same authors found that UTIs were responsible for a mortality rate of 2.3% [20]. In 2017, the European Centre

for Disease Prevention and Control (ECDC) also noticed a UTI emergence of 2% among the patients hosted in intensive care units for more than two days; 98% of these UTI episodes were associated with the use of a urinary catheter [21].

Urinary catheters are considered the most common indwelling devices. Currently, in the United States, over 30 million urinary catheters are inserted per year [22]. Previous studies carried out in several European and US hospitals reported about 15-25% of patients experiencing catheterization during their hospital permanence. The emergence of catheter-associated urinary tract infections (CAUTIs) is increasingly common, representing approximately 75% of hospital-acquired or nosocomial UTIs [23, 24]. Moreover, when compared to other 20 types of medical devices, catheters revealed an infection incidence of 33% [22]. The likelihood of developing CAUTIs increases with the duration of catheterization. Studies described that the incidence of CAUTIs among patients undergoing non-Foley or short-term urinary catheterization (< 7 days) was 10-50%, increasing to 90-100% in long-term catheterization (> 28 days) [25, 26].

Ureteral stents are also commonly used devices in modern urology practice. Like catheters, stents are very prone to contamination and colonization by different pathogens. Actually, 31% of the patients with ureteral stents develop UTIs [27], and 45–100% of patients have bacteriuria [28]. As with any biomedical device, exposure time is a risk factor for bacterial/fungal colonization. In fact, a previous research found that the incidence of stent colonization and bacteriuria increases from 69% in patients with temporary stents to 100% in patients carrying chronic indwelling stents [29].

Besides these alarming numbers, there is also an increasing cost associated with UTIs. In the United States, the problems related to UTIs have an estimated cost of \$1.6 - \$3.5 billion each year [30]. Regarding CAUTI, the annual treatment costs are over \$350 million [31] and £1–2.5 billion [32] in the United States and the United Kingdom, respectively. In relation to stent-associated UTI, the total economic costs are approximately \$15 per patient per day [33].

The successful treatment of catheter and stent-associated UTIs requires the background knowledge of the pathogens involved in the infection. Different microorganisms have been responsible for the colonization of UTDs. Some of the most commonly observed are *Escherichia coli*, *Staphylococcus aureus*, *Pseudomonas aeruginosa*, *Proteus* spp., *Klebsiella pneumoniae*, *Staphylococcus epidermidis*, *Enterococcus* spp., and *Candida* spp. [9, 34, 35]. These microorganisms commonly attach to indwelling medical devices, forming biofilms. These are complex three-dimensional (3D) structures composed by sessile microbial communities surrounded by a matrix of self-produced extracellular polymeric substances (EPS), including proteins, polysaccharides, nucleic acids, and molecules involved in cell-cell communication [36, 37].

Biofilm formation is, along with encrustation, the main reason why device-associated infections are considered so recalcitrant. Although they are two distinct phenomena generated by different factors, they can overlap and, consequently, worsen the infection. The development of new surface materials/techniques to overcome these infections requires the full comprehension of both phenomena.

Biofilm growth is governed by a number of physical, chemical and biological processes, and begins with the reversibly microbial adhesion to a conditioned surface either by physical forces or bacterial appendages (pili or flagella) [38]. Physical forces associated with this weak bacterial adhesion include van der Waals forces, as well as hydrophobic, steric and electrostatic interactions [39]. The rate of cell adhesion depends not only on the type and number of free-swimming cells, but also on the physicochemical characteristics of the material used in the implanted device, the fluid behaviour, and other environmental factors, such as temperature and pH [40]. When bacterial appendages overcome the physical repulsive forces [41], an irreversible attachment between bacterial surface structures and substratum occurs and microorganisms start to communicate with each other via quorum sensing by the production of autoinducer signals. In a maturation stage, a significant growth of the biofilm population occurs, with an increase of biofilm thickness up to 200

μm [42]. The final stage of biofilm development includes the detachment of bacteria, which may then colonize new areas [38].

Ureteral stents and urinary catheters are usually colonized both on extraluminal and intraluminal sides. While in an initial phase, biofilms are composed of single-species populations, in a further stage, multispecies communities are commonly detected. Overall, the chronicity of the infections associated with implanted biomedical devices is attributed to the growing resistance of the pathogens to antimicrobial agents, which is strongly related to the slow penetration of drugs within the EPS matrix, as well as the presence of persister cells that stay in a transitory dormant state and induce recurrent infections [43, 44]. The increasing antimicrobial resistance has limited the strategies to prevent and control UTIs.

Encrustation, on the other hand, results from the colonization of indwelling devices by urease-positive pathogens. Despite being mainly caused by *Proteus mirabilis* [45], other species can be involved in the formation of these encrustations, namely *Morganella morganii*, *P. aeruginosa*, *K. pneumoniae* and *Proteus vulgaris*. During the process of blockage, urease catalyzes the hydrolysis of urea into ammonia and carbamate, increasing urinary pH and, consequently, promoting stone formation by salt precipitation (calcium phosphate and struvite crystals) and potentially leading to complete occlusion of the catheter/stent through encrustation [46]. Apart from blocking the stent lumen, these encrustations potentiate further bacterial adhesion and biofilm formation, frequently resulting in complete device failure [47].

The complications associated with indwelling devices have been the main driving force for the development of alternative materials with antimicrobial and antifouling properties.

4. PDMS-BASED SURFACES TO PREVENT INFECTIONS IN URINARY TRACT DEVICES

In the last decades, a series of improvements have been performed in urinary catheters aiming to reduce pathogen colonization. As described in

previous sections, PDMS is prone to bacterial adhesion essentially due to its hydrophobic properties. In order to overcome this drawback, several coating strategies have been developed, conferring antimicrobial potential to PDMS or modifying its physicochemical properties, aiming to prevent bacterial adhesion and biofilm formation. Table 2 describes the antibiofilm strategies of different PDMS coatings and their potential against several bacterial and fungal species. PDMS coatings were grouped into four categories: (1) release of antimicrobial agents, (2) contact-killing, (3) anti-adhesive, and (4) biofilm architecture disruption.

Bactericidal/fungicidal strategies include the use of silver and antimicrobial agents or disinfectants (Table 2). Up to date, several studies have reported the effectiveness of silver/PDMS-coated catheters in the prevention and control of catheter-associated infections. The mechanisms of action of silver are already well characterized and include impairment of microbial membrane function by loss of membrane potential, protein dysfunction, and oxidative stress [8, 48]. Moreover, silver is one of the few antimicrobial agents approved by the Food and Drug Administration (FDA) for urinary catheter applications [8].

In the early 2000s, Ahearn et al. exploited the efficacy of silver/hydrogel-coated PDMS catheters against a broad range of microorganisms. Coated catheters reduced the adhesion by 73% for *Citrobacter diversus*, 65% for *Enterobacter cloacae*, 71-93% for *Enterococcus* spp., 70% for *E. coli*, 30% for *K. pneumoniae*, 70% for *P. mirabilis*, 92% for *P. aeruginosa*, and 96% for *Staphylococcus saprophyticus* compared to uncoated catheters [49]. Silver ions have also been applied as PDMS coatings, improving their potential against bacterial adhesion and biofilm growth [50]. Likewise, silver nanoparticles (AgNPs) decreased biofilm formation by *E. coli*, *P. mirabilis* and *K. pneumoniae*, preventing urinary tract infections [51]. Indeed, AgNPs are one of the most attractive types of catheter coatings. Dayyoub et al. prepared a PDMS hydrophobic film composed by tetraether lipids-coated silver nanoparticles distributed in poly(lactic-co-glycolic acid) loaded with norfloxacin, and tested it against a broad variety of bacterial species. In this study, adhered cells decreased about 48% on coated PDMS films compared to the uncoated PDMS [52]. In turn, Heidari

and co-workers evaluated silver/poly(p-xylylene)-coated catheters and observed a reduction in *E. coli* and *Staphylococcus cohnii* biofilms [53]. Recently, the efficacy of silver-polytetrafluoroethylene (Ag-PTFE) nanocomposites was evaluated against *E. coli*, *P. mirabilis* and *S. aureus*. Results showed that Ag-PTFE-coated catheters reduced bacterial adhesion and yielded strong antibiofilm activity (97%) [54, 55]. However, despite its broad-spectrum antimicrobial activity, silver-impregnated catheters can easily lose their properties in the long term and trigger bacterial resistance in intermittent catheterization [8].

Antimicrobial coatings were introduced as a good option to inhibit or delay the onset of biofilm formation. Up to date, several antimicrobial or disinfectant agents have been impregnated into silicone urinary catheters. In 2000, Simhi et al. demonstrated that PDMS impregnated with a secondary metabolite produced by *Myxococcus xanthus* significantly reduced the number of *E. coli* cells adhered to the surface [56]. Similar results were obtained for silicone catheters coated with gendine. This disinfectant was able to reduce the number of viable cells adhered to internal and external catheter surfaces, except for *P. aeruginosa* [57]. In turn, triclosan-coated catheters presented high resistance to encrustation and blockage by *P. mirabilis* and prevented the colonization by MRSA and carbapenemases-producing *E. coli* for 12 consecutive weeks [58, 59]. Rifampicin and sparfloxacin-coated catheters also prevented bacterial colonization [58].

In 2015, Gonçalves and co-workers showed the strong effect of PDMS coated with poly(catechin) conjugated with trimethoprim and sulfamethoxazole on the reduction of adhered Gram-negative and Gram-positive bacteria [60]. Likewise, the antimicrobial film composed by norfloxacin revealed a potent bactericidal activity, killing 99.9% of the adhered bacteria [52]. Lastly, Alves et al. proved that liposomal amphotericin B impregnated on silicone catheters reduced *Candida albicans* attachment by 3 Log CFU [21]. The success of this type of coating is usually attributed to the high-local concentrations of antimicrobial agents released at the potential site of colonization and their high effectiveness to target the pathogen [8]. Nevertheless, the continued

use of antimicrobial drugs may lead to bacterial resistance that compromises the application of these coatings [61].

In the last decade, antimicrobial peptides (AMPs) have emerged as contact-killing coatings for urinary catheters. This type of coating displays broad-spectrum activity targeting the pathogens through multiple pathways [8]. In 2014, Lim et al. described two arginine/lysine/tryptophane-rich antimicrobial peptides, RK1 and RK2. Catheters coated with these AMPs exhibited excellent antimicrobial activity towards *E. coli*, *S. aureus* and *C. albicans* [62]. *C. albicans* biofilm formation was also substantially inhibited (75-90%) by coumarin-linker-(ACHC- β 3hVal- β 3hLys)₃-loaded catheters [63]. The synthetic AMP CWR11 was able to reduce the bacterial attachment on a PDMS surface by 92% for *E. coli*, *P. aeruginosa* and *S. aureus* [64]. Recently, Lim et al. developed a new antimicrobial peptide (HHC36) into anhydrous polycaprolactone polymer-based dual-layer coated [PLC(P)-POPC(P)]. The coated PDMS catheters reduced bacterial adherence on catheter surfaces by 100% [65]. Although AMPs have a strong activity towards bacteria and fungi and low level of induced resistance compared to other antimicrobial agents, they may be toxic at high doses [61].

Since microbial adhesion depends on the charge, roughness and topography of the surface, anti-adhesive surfaces have optimised the physicochemical properties in order to prevent the initial microbial adhesion and thus reduce the biofilm development. Several polymers such as polyethylene glycol (PEG), hydrogels, zwitterionic polymers and cationic polymers have been applied as antifouling coatings for PDMS catheters. The polyethylene glycol capability to adsorb nonspecific proteins has been reported by several authors [8, 66, 67]. In 2001, Park et al. developed PEG-modified PDMS surfaces and evaluated them against *E. coli* and *S. epidermidis*. Bacterial adhesion decreased approximately 1 Log CFU on PDMS modified with monomethoxy poly(ethylene glycol) [68]. Despite PEG-coated materials are effectively resistant to nonspecific protein adsorption and short-term bacterial adhesion, this kind of coating has limited success in preventing biofilm formation [67]. Moreover, the

potential immunogenicity of PEG has also been reported as a relevant weakness [8].

Similarly to PEG, hydrogel coatings increase surface hydrophilicity, inhibiting nonspecific protein adsorption. In 2002, Park and co-workers demonstrated the antifouling efficacy of a new hydrogel based on poly(ethylene oxide)-poly(polytetramethylene oxide) copolymer-coated silicone catheter. The hydrogel-coated silicone catheter was able to extend the catheter patency up to 20 h versus 7.8 h with the control [69]. Recently, Yong et al. reported that the addition of a N-halamine monomer (a biocide) to the hydrogel coating deactivated both *E. coli* and *S. aureus* after 30 min of contact and reduced biofilm formation by 90% [70]. Moreover, Chung et al. in a prospective interventional study demonstrated the effectiveness of hydrogel-coated catheters in the prevention of CAUTIs [71].

Polyzwitterion coatings also resist to non-specific protein adsorption through electrostatic and steric repulsion [8]. In 2014, Diaz Blanco et al. developed a new coating based on PDMS grafted with gallic acid (GA), activated by laccases triggering the polymerization of zwitterionic sulfobetaine methacrylate monomers. Catheters coated with this film demonstrated a strong ability to resist bacterial adhesion and biofilm formation by *P. aeruginosa* and *S. aureus* [72]. Additionally, Vatterott et al. produced a new copolymer constituted by a 2-(dimethylamino)ethyl methacrylate derivate and poly(sulfobetaine methacrylate) (PTMAEMA-co-PSPE). Multilayer coatings on PDMS reduced *S. aureus* adhesion by 40% [73]. Sulfobetaine acrylamide covalently conjugated with polydopamine films-deposited copper ions coating also exhibited high fouling resistance and antimicrobial properties towards *E. coli* and *S. epidermidis*, as confirmed by the low number of adhered bacteria [74]. In turn, PDMS coated with a copolymer formed by polyacrylate [ethylene glycol dicyclopentenyl ether acrylate-co-di(ethyleneglycol) methyl ether methacrylate] was able to inhibit *E. coli* and *P. mirabilis* biofilm formation by up to 95% [75]. Based on these data, polyzwitterion coatings appear to be an effective anti-biofouling strategy.

Table 2. Antibiofilm coatings applied on PDMS-based urinary catheters

Antibiofilm strategy	Coating	Species	Major conclusions	Year	Reference
Bactericidal/ Fungicidal	Silver Hydrogel/silver	<i>C. diversus</i> <i>E. cloacae</i> <i>E. faecalis</i> <i>E. faecium</i> <i>E. coli</i> <i>K. pneumoniae</i> <i>P. mirabilis</i> <i>P. aeruginosa</i> <i>S. saprophyticus</i>	Mean percentage reduction of adhesion to hydrogel/silver-silicone catheters versus silicone catheters was 72.5% for <i>C. diversus</i> , 64.6% for <i>E. cloacae</i> , 70.6-92.5% for <i>Enterococcus</i> spp., 70.3% for <i>E. coli</i> , 30.1% for <i>K. pneumoniae</i> , 70.3% for <i>P. mirabilis</i> , 91.8% for <i>P. aeruginosa</i> , and 95.5% for <i>S. saprophyticus</i> .	2000	[49]
	Silver	<i>E. coli</i> <i>K. pneumoniae</i> <i>P. mirabilis</i>	Silver-coated catheters significantly decreased bacterial adhesion (ratio of means: 0.63, $p = 0.0083$) and biofilm formation (ratio of means: 3.01, $p = 0.0488$) when compared to non-silver-coated catheters.	2015	[50]
	Silver nanoparticles	<i>K. pneumoniae</i> <i>P. mirabilis</i>	Silver-coated catheters decreased biofilm formation by 6 Log for <i>E. coli</i> on day 10 ($p = 0.032$); 4 Log for <i>P. mirabilis</i> ($p = 0.003$) and 1 Log for <i>K. pneumoniae</i> , both on day 14 ($p = 0.036$).	2016	[51]
	Silver with poly(p-xylylene)	<i>E. coli</i> <i>S. cohnii</i>	The supernatant of the silver/poly(p-xylylene)-coated catheters significantly reduced biofilm formation, similar to the antibiotic control (penicillin-streptomycin).	2017	[53]
	Tetraether lipids-coated silver nanoparticles distributed in a hydrophobic film of poly(lactic-co-	<i>E. coli</i> <i>P. aeruginosa</i> <i>P. mirabilis</i> <i>S. aureus</i>	Adhered cells decreased about 48% on coated silicone films compared to the control.	2017	[52]

Antibiofilm strategy	Coating	Species	Major conclusions	Year	Reference
Bactericidal/ Fungicidal	Silver glycolic acid) loaded with norfloxacin Silver-polytetrafluoroethylene nanocomposites	<i>S. epidermidis</i> <i>E. faecalis</i> <i>E. coli</i> <i>S. aureus</i> <i>P. mirabilis</i>	The Ag-PTFE-coated catheters reduced bacterial adhesion and exhibited strong antibiofilm activity (97.4%) compared with the silicone catheters. Coated catheters resisted encrustation to 78 ± 5.66 h and 89.5 ± 3.54 h with an initial concentration of 10^6 and 10^3 cells/mL in the bladder, respectively, versus 33.3 ± 1.1 h and 36.2 ± 1.1 h achieved by control catheters.	2019	[54, 55]
	Antimicrobial agents/Disinfectants Macrocyclic secondary metabolite produced by <i>M. xanthus</i>	<i>E. coli</i>	The secondary metabolite significantly reduced the number of adhered bacteria on the silicone surface (approximately less 7.0×10^6 cell/cm ² compared to control).	2000	[56]
	Gendine (a combination of Gentian Violet and chlorhexidine)	<i>E. coli</i> <i>P. aeruginosa</i> MRSA <i>C. parapsilosis</i> <i>P. mirabilis</i>	The gendine-coated catheters significantly reduced the number of viable organisms adhering to their internal and external surfaces, except for <i>P. aeruginosa</i> , when compared to the uncoated control ($p < 0.01$).	2005	[57]
	Hydrogel impregnated with triclosan, iodine and polyhexamethylene biguanide	<i>P. mirabilis</i>	Only catheters containing triclosan showed enhanced resistance to encrustation and blockage by <i>P. mirabilis</i> (up to > 7 days).	2010	[59]
	Poly(catechin) conjugated with trimethoprim and sulfamethoxazole	<i>E. coli</i> <i>P. aeruginosa</i> <i>P. mirabilis</i> <i>S. aureus</i>	The most significant reduction in adhesion was observed with poly(catechin)-TMP (85% for Gram-negative and 87% for Gram-positive bacteria) and with poly(catechin)-TMP-SMZ (85% for Gram-negative and 91% for Gram-positive bacteria).	2015	[60]

Table 2. (Continued)

Antibiofilm strategy	Coating	Species	Major conclusions	Year	Reference
Bactericidal/ Fungicidal	Antimicrobial agents/Disinfectants				
	Tetraether lipids-coated silver nanoparticles distributed in a hydrophobic film of poly (lactic-co-glycolic acid) loaded with norfloxacin	<i>S. epidermidis</i> <i>B. subtilis</i> <i>E. coli</i> <i>P. aeruginosa</i> <i>P. mirabilis</i> <i>S. aureus</i> <i>S. epidermidis</i> <i>E. faecalis</i>	The antimicrobial film killed 99.952% of the adhered bacteria.	2017	[52]
	Rifampicin, triclosan and sparfloxacin Liposomal amphotericin B	<i>E. coli</i> (NDM-1) MRSA <i>C. albicans</i>	Antimicrobial urinary catheter prevented colonisation by MRSA and carbapenemases-producing <i>E. coli</i> for 12 weeks. L-AmB immobilized reduced fungal attachment by approximately 3 Log.	2019 2019	[58] [21]
Contact-killing	Antimicrobial peptide (AMP)				
	Arginine/lysine/tryptophane-rich antimicrobial peptides: RK1 (RWKRWRRKK) and RK2 (RKKRWRRKK)	<i>E. coli</i> <i>S. aureus</i> <i>C. albicans</i>	The peptide-coated silicone surfaces exhibited excellent microbial killing activity towards bacteria and fungi (> 70%).	2014	[62]
	Synthetic antimicrobial peptide: CWR11 (CWFWKWRRRRR-NH2)	<i>E. coli</i> <i>P. aeruginosa</i> <i>S. aureus</i>	Bacterial attachment on the PDMS-CWR11 surface was significantly reduced by 92%.	2015	[64]
Coumarin-linker-(ACHC-β3hVal-β3hLys)3 (β-peptide 1)	<i>C. albicans</i>	B-peptide-loaded catheters substantial reduced <i>C. albicans</i> biofilm formation by 75-90%.	2016	[63]	

Antibiofilm strategy	Coating	Species	Major conclusions	Year	Reference
Contact-killing	Antimicrobial peptide (AMP) Antimicrobial peptides (HHC36) into anhydrous polycaprolactone (PCL) polymer-based dual layer coating PCL(P)-POPC(P)	<i>E. coli</i> <i>P. aeruginosa</i> <i>S. aureus</i>	The PCL(P)-POPC(P)-coated silicone urinary catheters significantly inhibited planktonic bacteria and reduced bacteria adherence on catheter surface by 100%.	2018	[65]
Anti-adhesive	Poly(ethylene glycol) (PEG) Monomethoxy poly(ethylene glycol) (MPEG) grafts	<i>E. coli</i> <i>S. epidermidis</i>	Bacterial adhesion significantly decreased after PDMS-based polyurethanes were modified with monomethoxy PEG (from 4.0×10^4 to 5.0×10^3 CFU/cm ²).	2001	[68]
	Hydrogel Hydrogel (multiblock copolymer) based on poly(ethylene oxide)-poly(polytetramethylene oxide) copolymer	<i>P. mirabilis</i>	The performance of the hydrogel-coated silicone catheter was extended up to 20 ± 3.1 h versus 7.8 ± 3.1 h with the control.	2002	[69]
	Hydrogel impregnated with N-halamine monomer	<i>E. coli</i> <i>S. aureus</i>	The addition of a biocidal N-halamine monomer to the hydrogel coating deactivated both <i>S. aureus</i> and <i>E. coli</i> within 30 min of contact and reduced biofilm formation by 90%.	2019	[70]
	Polyzwitterion PDMS was plasma-activated and preaminated, allowing subsequent laccase-catalyzed grafting of the natural phenolic compound GA.	<i>P. aeruginosa</i> <i>S. aureus</i>	Biofilm formation on PDMS-coated samples was reduced by about 80% compared to the <i>P. aeruginosa</i> biofilm produced on the urethra part of uncoated catheters, and by about 90% in the case of <i>S. aureus</i> biofilm produced on the catheter balloon.	2014	[72]

Table 2. (Continued)

Antibiofilm strategy	Coating	Species	Major conclusions	Year	Reference
Anti-adhesive	<p>Polyzwitterion</p> <p>The tethered GA residues were activated by laccases to phenoxy radicals, triggering an enzymatically initiated radical polymerization of zwitterionic sulfobetaine methacrylate monomers.grafting of the natural phenolic compound GA. The tethered GA residues were activated by laccases to phenoxy radicals, triggering an enzymatically initiated radical polymerization of zwitterionic sulfobetaine methacrylate monomers.</p>				
	<p>PTMAEMA-co-PSPE</p> <p>Polyacrylate [ethylene glycol dicyclopentenyl ether acrylate - co-di(ethyleneglycol) methyl ether methacrylate]</p>	<p><i>S. aureus</i></p> <p><i>E. coli</i></p> <p><i>P. mirabilis</i></p>	<p>Multilayer films not only reduced the bacterial adhesion by 40% relative to uncoated PDMS, but also killed the bacteria adhered to the surface.</p> <p>Coated PDMS inhibited <i>E. coli</i> and <i>P. mirabilis</i> biofilms by up to 95% when compared with uncoated PDMS after 10 days of continuous bacterial exposure.</p>	<p>2016</p> <p>2017</p>	<p>[73]</p> <p>[75]</p>

Antibiofilm strategy	Coating	Species	Major conclusions	Year	Reference
Anti-adhesive	<p>Polyzwitterion</p> <p>Copper ions deposited on polydopamine films with covalent conjugation of sulfobetaine acrylamide (pDA-SBAA)</p>	<p><i>E. coli</i></p> <p><i>S. epidermidis</i></p>	<p>r-pDA-SBAA coatings exhibited fouling resistance and antimicrobial properties which were confirmed by low adherent bacterial numbers ($\approx 1 \times 10^5$ cell/cm²) and high dead fraction (0.8).</p>	2019	[74]
	<p>Cationic polymers</p> <p><i>N</i>-acetyl-d-glucosamine-1-phosphate acetyltransferase inhibitors plus protamine sulphate</p>	<p><i>P. aeruginosa</i></p> <p><i>S. epidermidis</i></p>	<p>Confocal microscopy confirmed that coated-silicone catheters were almost free from bacterial colonization.</p>	2006	[76]
	<p>Polydopamine- poly(2-methacryloyloxyethyl)trimethylammonium chloride (pDA-g-pMTAC)</p>	<p><i>E. coli</i></p> <p><i>P. aeruginosa</i></p>	<p>The pDA-g-pMTAC-coated catheters showed a significant reduction in bacterial adhesion (50% for <i>E. coli</i> and 90% for <i>P. aeruginosa</i>).</p>	2016	[77]
Antifouling	<p>Cationic polymers</p> <p>Isobornyl methacrylate/diethylene glycol ethyl ether methacrylate (IBMA/DEGMA) (3-acrylamidopropyl) trimethylammonium chloride (AMPTMA) with trimethylammonium chloride (AMPTMA)</p>	<p><i>E. coli</i></p> <p><i>P. aeruginosa</i></p> <p><i>S. aureus</i></p>	<p>IBMA/DEGMA polymer demonstrated a bacterial coverage of less than 0.5%.</p>	2016	[78]

Table 2. (Continued)

Antibiofilm strategy	Coating	Species	Major conclusions	Year	Reference
Antifouling	<p>Cationic polymers with quaternized polyethylenimine methacrylate (Q-PEI-MA) together with (polyethylene glycol dimethacrylate, PEGDMA)</p>	<p><i>E. coli</i> <i>P. aeruginosa</i> <i>S. aureus</i> MRSA VRE</p>	<p>AMPTMA/PEGDMA film coating exhibited good antibiofilm and antimicrobial effect against MRSA, with 99.4% <i>in vitro</i> reduction and 98.9% <i>in vivo</i> reduction. AMPTMA/PEGDMA/Q-PEI-MA film coating had significant efficacy against VRE, with 96.8% <i>in vitro</i> reduction and 94.5% <i>in vivo</i> reduction.</p>	2017	[79]
	<p>Dodecyl methacrylate/poly(ethylene glycol) methacrylate-and an acrylic acid (Poly(DMAmPEGMA-AA))</p>	<p><i>E. coli</i> <i>S. aureus</i></p>	<p>Polymer-coated surface displayed significantly reduced attachment of bacteria (> ~8-fold) compared to the non-coated substrates.</p>	2017	[80]
	<p>Other polymers Calixarene polymer</p>	<p><i>E. coli</i> <i>P. mirabilis</i></p>	<p>Biofilm formation was significantly reduced in the coated silicone samples compared to uncoated control ($p = 0.02$).</p>	2018	[81]
Disruption of biofilm architecture	<p>Enzymes for EPS disruption Acyase and α-amylase</p>	<p><i>E. coli</i> <i>P. aeruginosa</i> <i>S. aureus</i></p>	<p>Assembly of both enzymes in hybrid nanocoatings resulted in stronger biofilm inhibition (30%) under both static and dynamic conditions. The quorum quenching and matrix-degrading enzyme assemblies delayed biofilm growth up to 7 days.</p>	2015	[82]
	<p>Acyase</p>	<p><i>P. aeruginosa</i></p>	<p>Biofilm formation was inhibited by 80% in the balloon part, while the urethra part inserted into the bladder model was able to inhibit biofilm formation by 45%.</p>	2015	[83]

Table 3. Antibiofilm coatings applied on PDMS-based ureteral stents

Antibiofilm strategy	Coating	Species	Major conclusions	Year	Reference
Bactericidal	Silver Silver and hydrogel	<i>E. coli</i> <i>E. faecalis</i>	The surface material had no direct influence on bacterial adhesion.	1997	[84]
	Tetraetherlipid-silver nanoparticle-norfloxacin-poly lactide coating (TANP)	<i>E. coli</i> <i>P. aeruginosa</i> <i>S. aureus</i> <i>S. epidermidis</i> <i>E. faecalis</i>	TANP-coated samples displayed a reduction in the precipitate concentration (> 20%) and biofilm volume (80%).	2018	[85]
Antifouling	PEG Mimics mussel adhesive protein conjugated to polyethylene glycol (mPEG-DOPA3)	<i>E. coli</i> <i>P. mirabilis</i> <i>E. faecalis</i>	The mPEG-DOPA3 coating significantly resisted the attachment of all uropathogens tested, with a maximum 231-fold reduction in adherence compared to uncoated disks.	2008	[86]
Anti-encrustation	Hydrophilic polymers Phosphoryl-choline	<i>P. mirabilis</i>	PC-coated stents showed lower encrustation compared with uncoated stents. PC-coating did not reduce microbial colonization or encrustation of the surfaces of these devices. There was some evidence that PC-coating makes these devices less vulnerable to these processes.	2002	[87]

Cationic polymers can also be anti-adhesive coating agents. Contrary to what was described before, this type of coating adsorbs both proteins and bacterial cells by attraction through the negatively charged bacterial membrane, exerting an anti-adhesive and antimicrobial effect [8]. Burton et al. developed a coating of *N*-acetyl-d-glucosamine-1-phosphate acetyltransferase inhibitors with protamine sulphate and evaluated its efficacy against *P. aeruginosa* and *S. epidermidis*. In this study, the coated silicone catheters were almost free of bacteria [76]. Likewise, the polydopamine-poly (2-methacryloxyethyl) trimethylammonium chloride showed a significant reduction in bacterial adhesion of 50% for *E. coli* and 90% for *P. aeruginosa* [77]. Adlington et al. demonstrated that the cationic polymer IBMA/DEGMA-coated PDMS displayed a bacterial coverage of less than 0.5% for *E. coli*, *P. aeruginosa* and *S. aureus* [78]. Recently, Zhou and colleagues developed two methacrylate polymers with excellent *in vitro* and *in vivo* antibiofilm and antimicrobial activities [79]. Lastly, poly(DMAmPEGMA-AA)-coated PDMS surfaces significantly inhibited bacterial attachment by 8 Log CFU compared to uncoated surfaces [80]. Another type of polymers, such as calixarene polymers, were reported as effective coatings to prevent biofilm formation by *E. coli* and *P. mirabilis* on PDMS surfaces [81].

Currently, different strategies are emerging aiming to disrupt the architecture of biofilm through matrix degradation or quorum sensing interruption. A study conducted by Ivanova et al. demonstrated the potential of acylase and α -amylase enzymes against extracellular polymeric substances. Assembly of both enzymes in hybrid coatings resulted in a strong biofilm inhibition (about 30%) for *E. coli*, *P. aeruginosa*, and *S. aureus*. Moreover, the quorum quenching and matrix-degrading enzymes delayed biofilm growth up to 7 days [82]. The same authors showed that acylase-coated PDMS catheters inhibited *P. aeruginosa* biofilm formation by 80% in the balloon part of the catheter, and by 40% into the urethra part [83]. These results revealed that enzymatic catheter coatings are promising to inhibit or delay biofilm formation.

Unlike in urinary catheters, antibiofilm coatings for ureteral stents were less exploited. Table 3 lists antibiofilm strategies based on distinct PDMS coatings and their effectiveness against several bacterial species. In 1997, Cormio et al. verified that PDMS stents coated with silver/hydrogel had no

direct influence on bacterial adhesion [84]. However, Frant et al. recently developed a new tetraetherlipid-silver nanoparticle-norfloxacin-poly lactide (TANP) coating and tested its antibiofilm potential towards *E. coli*, *P. aeruginosa*, *S. aureus*, *S. epidermidis*, and *E. faecalis*. TANP-coated stents reduced the precipitate concentration on silicone surfaces by up to 20% and the biofilm volume decreased 80%, showing the effectiveness of the coatings [85].

In 2008, Ko et al. introduced a new approach inspired in marine mussels to prevent biofilm formation. The biomimetic mussel adhesive protein conjugated to polyethylene glycol coating significantly resisted attachment of uropathogens, with a maximum 231-fold reduction in adherence compared to the control [86]. Lastly, the application of hydrophilic polymers such as phosphoryl-choline on silicone stents did not reduce microbial colonization or encrustation [87].

Although a wide range of antibiofilm coatings for PDMS-based urinary devices is currently available, there is a growing need to develop new effective and stable coatings to prevent or delay biofilm formation.

The development of biomimetic polymeric superhydrophobic surfaces generated an increasing interest due to their outstanding anti-biofouling properties. A strategy to combat microbial biofouling consists in modifying the topographical structure of the surface at nanometer to micrometer levels avoiding cell attachment, colonization and, ultimately, biofilm formation. Some authors, inspired on the nature, physically modified surfaces creating micropatterns to control the hydration layer and turn them superhydrophobic. This technology allows the development of surfaces that mimic the texture of shark skin or the self-cleaning properties of lotus leaves [88, 89]. In 2014, Bixler and co-workers produced PDMS-microstructured surfaces inspired by rice leaves and butterfly wings, and tested their anti-biofouling effectiveness against *E. coli*. Data demonstrated that the modified surface resulted in a coverage area reduction of 28%, suggesting the importance of surface geometrical features on fouling resistance [90]. Although these novel bioinspired surfaces have shown promising antifouling activity, their application in the medical field and,

particularly, in the construction of urinary tract devices needs further research.

5. FLOW SYSTEMS FOR SURFACE EVALUATION

A wide variety of *in vitro* biofilm model systems have been established to evaluate the efficacy of antimicrobial and antifouling surfaces under flow conditions. Indeed, this type of experimental set-up is more advantageous compared with static experiments, allowing a better representation of the hydrodynamic conditions that occur in different parts of the human body. Furthermore, it is well known that fluid flow affects not only cell adherence to the surface material, but also biofilm formation and its structure [91]. In this section, we briefly summarize the commonly used platforms for the *in vitro* assessment of cell adhesion and biofilm formation under flow conditions, with an emphasis on two types of flow systems - the modified Robbins device (MRD) and the parallel plate flow chamber (PPFC) [92-94]. Each reactor presents advantages and disadvantages that must be considered before use.

5.1. Drip Flow Reactor

The drip flow reactor has been used to mimic the flow inside indwelling medical devices and to evaluate potential antimicrobial materials [95, 96]. These reactors consist in a device with four completely separate parallel chambers with vented lids (each chamber contains a coupon where the biofilm can form) and are recommended for visualization and quantification of biofilms formed at low shear stress conditions [97]. These reactors require small space, are easy to operate, and allow noninvasive sample analysis. However, they present some disadvantages as the low number of sampling surfaces and the heterogeneity of biofilm development on the coupons due to hydrodynamics [98].

5.2. Rotary Biofilm Reactors

Three different types of rotary biofilm reactors are also commonly used in the assessment of material and fluid flow effects on biofilm development: the rotary annular reactor, the rotary disk reactor and the concentric cylinder reactor. These reactors have different designs. The rotary annular reactor is composed by a stationary outer cylinder and a rotating inner cylinder whose rotation frequency can be controlled so that a well-mixed liquid phase, turbulent flow and constant shear stress fields may be obtained [99]. The rotary disk reactor contains a disk that holds several coupons and is connected to a magnet that allows the regulation of the rotational speed [100]. The concentric cylinder reactor is composed of four cylindrical sections that can be rotated at variable speeds within four concentric chambers [101]. The last one can be used to test different cell suspensions, since each chamber of the concentric cylinder reactor contains independent feeding and sampling ports. The primary limitation of these reactors is related to the low number of individual strains that can be tested simultaneously (one microorganism per experiment in the rotary annular reactor and disk reactor, and up to four in the concentric cylinder reactor).

5.3. Microfluidics

Microfluidics can also be used to demonstrate the combined effect of several factors on the development of medically relevant biofilms [102-104]. Microfluidic systems allow the precise manipulation of the fluid contained in the microchannels, and their main advantages include the low volume requirements, the precise gradient generation, the easy handling due to their small dimensions, and the capacity to mimic microscale events, such as drug delivery systems [105-107].

5.4. Flow Cells

Flow cells have been widely used to study bacterial cell adhesion and biofilm formation under hydrodynamic conditions that mimic the urinary tract [92, 108, 109]. Originally developed by Jim Robbins and Bill McCoy, and later patented by the Shell Oil Company, the Robbins device consists of a tube incorporating several threaded holes where different coupons are fixed on the end of screws placed into the liquid stream. These coupons are parallel aligned to the fluid flow and can be independently removed to be further analyzed [110, 111]. MRD is a new version of the original Robbins device that is essentially composed by a square-channel tube with equally-spaced sampling plugs where the coupons are mounted without disturbing the flow characteristics [112]. It has an entry section long enough to allow the flow to stabilize before reach the coupons and, consequently, a constant shear stress is maintained along all the platform [113], which is extremely important to minimize the differences between the coupons. In fact, it is well known that the transport rate of oxygen, cells and nutrients to the coupon surface is strongly dependent on the fluid hydrodynamics [114]. Moreover, it can support biofilm growth for several weeks without stoppage, which constitutes an important advantage of the MRD over the original Robbins device [115, 116]. Our research group has been using a custom-made semi-circular flow cell whose hydrodynamics was fully characterized by computational fluid dynamics (CFD) [117], and which can be operated at low or high flow rates in order to mimic the biofilms formed in medical devices or industrial pipes and equipment, respectively [115, 117]. This flow cell was constructed so as to have an enough inlet length for full flow development, and a large surface area on which the hydrodynamic conditions remain constant for a wide range of flow velocities. The flow cell system is mainly composed by a recirculating tank, one vertical semi-circular flow cell (about a meter high), and peristaltic and centrifugal pumps.

5.6. Parallel Plate Flow Chamber

Contrary to the flow systems previously described, the PPFC was designed to allow real-time observation of microbial adhesion and biofilm development. Several authors have frequently applied PPFCs to monitor biofilm formation [118, 119]. This platform can contain one or two glass viewing ports that enable the use of a microscope and a camera for image capture and further monitorization of bacterial adhesion to the material. PPFCs are usually smaller than flow cells and cheaper to build. They can also be used to conduct experiments in parallel under the same operational conditions, which enables a higher throughput.

6. ADHESION AND BIOFILM FORMATION IN URINARY CATHETERS AND URETERAL STENTS: EXPERIMENTAL APPROACH

A PPFC was used in this work to evaluate the transition from initial *E. coli* adhesion to the complex structure of the biofilm formed on PDMS, one of the most widely used materials for the manufacture of UTDs. This *in vitro* flow system was fully characterized by CFD [92] and showed to be adequate to mimic the flow conditions found in different biomedical systems [120, 121], including urinary catheters and ureteral stents. The numerical simulations revealed that the average shear strain rate value of 15 s^{-1} reported for urinary flow in catheters [122] can be attained in the PPFC system at a flow rate of 2 mL/s. On the other hand, shear stress values between 0.01 and 0.038 Pa were described for problematic zones in ureteral stents [123]. The average shear stress in critical areas that are prone to encrustation (0.024 Pa) can be obtained by operating the PPFC system at a flow rate of 4 mL/s. Therefore, the PPFC was selected for this study because it can replicate relevant hydrodynamic conditions of UTDs and allows direct observation of bacterial adhesion to PDMS in real-time by conventional light *microscopy*, as well as offline monitoring of biofilm development on the same substrate.

6.1. PPFC System

The PPFC system used in the present work is represented in Figure 1. The flow chamber had a rectangular cross section of 0.8×1.6 cm and a length of 25.4 cm, and contained a bottom and a top opening for the introduction of the test surfaces. This setup generated a window of 6.7×1.6 cm through which bacterial adhesion within the chamber may be visualized. The PPFC was coupled to a jacketed glass tank connected to a centrifugal pump and a valve by a silicone tubing system. The valve allowed the bacterial suspension to circulate through the system at a controlled flow rate, in this case, 2 or 4 mL/s in order to obtain wall shear forces similar to those found in urinary catheters or ureteral stents, respectively. A recirculating water bath was connected to the tank jacket to enable temperature control at 37°C to mimic human body conditions.

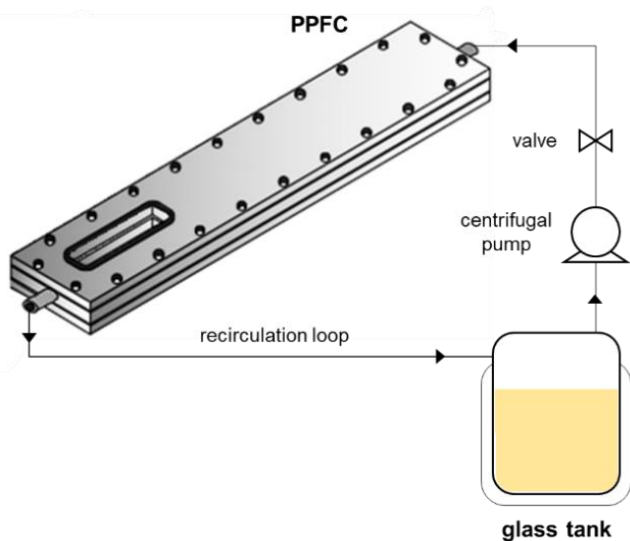


Figure 1. Schematic representation of the PPFC system.

Before performing adhesion or biofilm formation assays, the PPFC system was sterilized by recirculating a sodium hypochlorite solution (3% v/v, 3 cycles of 15 min each). Then, it was washed with sterile water and placed inside a laminar flow chamber for 30 min of UV sterilization. All

the surfaces (glass microscopic slides for the top and PDMS slides for the bottom of the PPFC) were sterilized by spraying with absolute ethanol for 5 min.

6.2. Synthesis and Thermodynamic Characterization of PDMS

The PDMS surfaces were prepared according to the procedure fully described by Moreira et al. [92]. Briefly, glass microscope slides ($W \times D \times H = 76 \times 26 \times 1$ mm, VWR) were washed with a commercial detergent (Sonasol Pril, Henkel Ibérica SA) and immersed in a sodium hypochlorite solution. The clean slides were then coated with PDMS. The PDMS (Sylgard 184 Part A, Dow Corning) was first submitted to an ultrasound treatment to eliminate air bubbles. The curing agent (Sylgard 184 Part B, Dow Corning) was added to the PDMS at a 1:10 ratio and the mixture was deposited as a thin layer (with a uniform thickness of 10 μm) on the top of glass slides by spin coating.

Surface and bacterial hydrophobicity (ΔG_{sws}^{TOT} and ΔG_{bwb}^{TOT} , respectively) were evaluated according to the approach of van Oss et al. [124-126]. The contact angles were determined by the sessile drop method in a contact angle meter (Dataphysics OCA 15 Plus, Germany) using water, formamide and α -bromonaphtalene as reference liquids. In this approach, the ΔG values can be calculated from the surface tension components by Equation (1):

$$\Delta G^{TOT} = -2 \left(\sqrt{\gamma_s^{LW}} - \sqrt{\gamma_w^{LW}} \right)^2 + 4 \left(\sqrt{\gamma_s^+ \gamma_w^-} + \sqrt{\gamma_s^- \gamma_w^+} - \sqrt{\gamma_s^+ \gamma_s^-} - \sqrt{\gamma_w^+ \gamma_w^-} \right) \quad (1)$$

If $\Delta G^{TOT} < 0$ mJ/m², the material is considered hydrophobic; if $\Delta G^{TOT} > 0$ mJ/m², the material is hydrophilic.

The free energy of adhesion between a surface and bacteria (ΔG_{bws}^{TOT}) can be calculated by Equation (2):

$$\Delta G_{bws}^{TOT} = \gamma_{sb}^{LW} - \gamma_{sw}^{LW} - \gamma_{bw}^{LW} + 2 \left[\sqrt{\gamma_w^+} (\sqrt{\gamma_s^-} + \sqrt{\gamma_b^-} - \sqrt{\gamma_w^-}) + \sqrt{\gamma_w^-} (\sqrt{\gamma_s^+} + \sqrt{\gamma_b^+} - \sqrt{\gamma_w^+}) - \sqrt{\gamma_s^+ \gamma_b^-} - \sqrt{\gamma_s^- \gamma_b^+} \right] \quad (2)$$

Thermodynamically, if $\Delta G_{bws}^{TOT} < 0$ mJ/m², adhesion is favored, while adhesion is not expected to occur if $\Delta G_{bws}^{TOT} > 0$ mJ/m².

Table 4. Contact angles with water (θ_w), formamide (θ_F) and α -bromonaphthalene (θ_B), surface tension parameters, free energy of interaction (ΔG_{sws}^{TOT} or ΔG_{bwb}^{TOT}) of the bacteria (*b*) and surface (*s*) when immersed in water (*w*), and free energy of adhesion (ΔG_{bws}^{TOT}) between the bacteria and the surface

	Contact angle (°)			Surface tension parameters (mJ/m ²)				Hydrophobicity (mJ/m ²)	Free energy of adhesion (mJ/m ²)
	θ_w	θ_F	θ_B	γ^{LW}	γ^+	γ^-	γ^{AB}	ΔG_{sws}^{TOT} or ΔG_{bwb}^{TOT}	ΔG_{bws}^{TOT}
<i>Surface</i>									
PDMS	113.6 ± 0.6	111.2 ± 0.6	87.6 ± 1.8	12.0	0.0	4.5	0.0	-61.8	32.6
<i>Bacteria</i>									
<i>E. coli</i>	19.1 ± 0.9	73.3 ± 0.7	58.5 ± 2.0	25.7	0.0	123.2	0.0	121.9	n/a

Note: n/a - not applicable.

Values are means ± SDs of three independent experiments.

Table 4 presents the results of the thermodynamic analysis of PDMS coating and *E. coli* cells based on contact angle measurements. It was observed that PDMS is hydrophobic ($\Delta G^{TOT} < 0$ mJ/m²), whereas *E. coli* cells are hydrophilic ($\Delta G^{TOT} > 0$ mJ/m²). From the water contact angle (θ_w , Table 4), PDMS can also be classified as non-wettable since θ_w exceeded 110° [127]. Regarding the polar surface components (γ^+ and γ^-), results showed that PDMS and *E. coli* cells have monopolar surfaces, being electron donors. From a thermodynamic point of view (Table 4), the

adhesion of *E. coli* to PDMS was not expected to occur ($\Delta G_{bws}^{TOT} > 0$ mJ/m²).

6.3. Initial Adhesion Assays

For the adhesion assays, the PPFC was mounted in a microscope (Nikon Eclipse LV100, Japan) to monitor cell attachment to PDMS in real-time during 25 min. An *E. coli* JM109(DE3) suspension of 7.6×10^7 cells/mL in citrate buffer 0.05 M was prepared and recirculated through the PPFC system at 2 or 4 mL/s. Citrate buffer was used to avoid any surface conditioning effects that may arise with using conventional culture medium. Images were acquired every 60 s with a camera (Nikon DS-Ri 1, Japan) connected to the microscope. The microscopic images were analyzed by ImageJ software (version 1.38e) to determine the number of adherent cells per square centimeter at each time point for each tested flow rate.

Figure 2 shows the initial adhesion results obtained for PDMS for each flow rate (2 and 4 mL/s). It is possible to observe that the number of adhered cells increased with time for both flow rates, having achieved an average value of 1.15×10^6 cells/cm² after 25 min of experiment. Moreover, the number of adhered cells was mostly similar between flow rates during the experimental time ($P > 0.05$ for 92% of the time points). Indeed, the initial adhesion rates (IAR) obtained from linear regression of the data presented in Figure 2 were very similar: 4.25×10^4 cells/(cm² s) for the flow rate of 2 mL/s and 3.83×10^4 cells/(cm² s) for the flow rate of 4 mL/s. Usually, increased flow velocities result in higher adhesion due to the increased cell transport to the surface [128]. However, it was not surprising that doubling the flow rate did not increase the number of attached cells because the higher shear forces may have contributed to higher cell detachment or be high enough to hamper the process of initial reversible adhesion [92, 129].

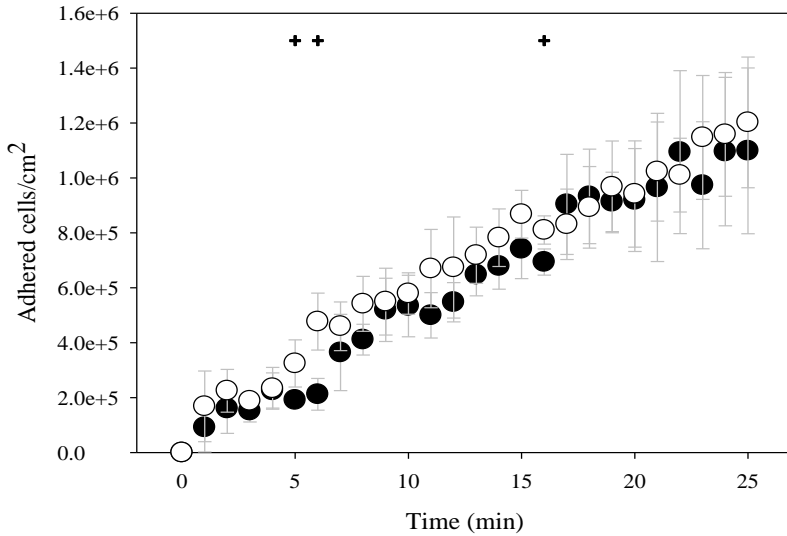


Figure 2. *E. coli* adhesion to PDMS surface at a flow rate of 2 mL/s (●; mimicking urinary catheters) and 4 mL/s (○; mimicking ureteral stents). The means \pm standard deviations (SDs) for three independent experiments for each condition are illustrated. Statistically significant differences for a confidence level greater than 95% ($P < 0.05$) are indicated by +.

6.4. Biofilm Formation Assays

Biofilm formation experiments using the PPFC system previously described (Section 6.1) were carried out for 24 h. Note that it has been reported that biofilms developed in UTDs are completely mature after 24 h [130]. Synthetic urine was the culture medium chosen to prepare the *E. coli* suspension [109], which recirculated through the PPFC at 2 and 4 mL/s in order to mimic the urine flow behaviour in urinary catheters and ureteral stents, respectively. After 24 h of biofilm growth, the PPFC was opened and the cells adhered on PDMS were removed through the swabbing method [131].

The total number of sessile cells on PDMS was determined by epifluorescence microscopy by staining the biofilm suspension with 4'-diamidino-2-phenylindole (DAPI; Merck, Germany) [132], while the cell culturability was assessed by spreading the biofilm suspension on plate

count agar (PCA, Oxoid, England) and incubating at 37°C for colony-forming unit (CFU) enumeration. Results of total and culturable cell quantification for both hydrodynamic conditions are shown in Figure 3. There were no statistically significant differences in the number of total and culturable cells between the two flow rates ($P > 0.05$). The 24-h biofilms formed on PDMS slides had on average 1.2×10^8 total cells/cm² and about 26% of these cells were culturable, regardless of the flow rate tested. These first results seem to indicate that the similar cell amount in *E. coli* biofilms developed under two different flow rates could be associated with the similar initial adhesion rates also obtained (Figure 2).

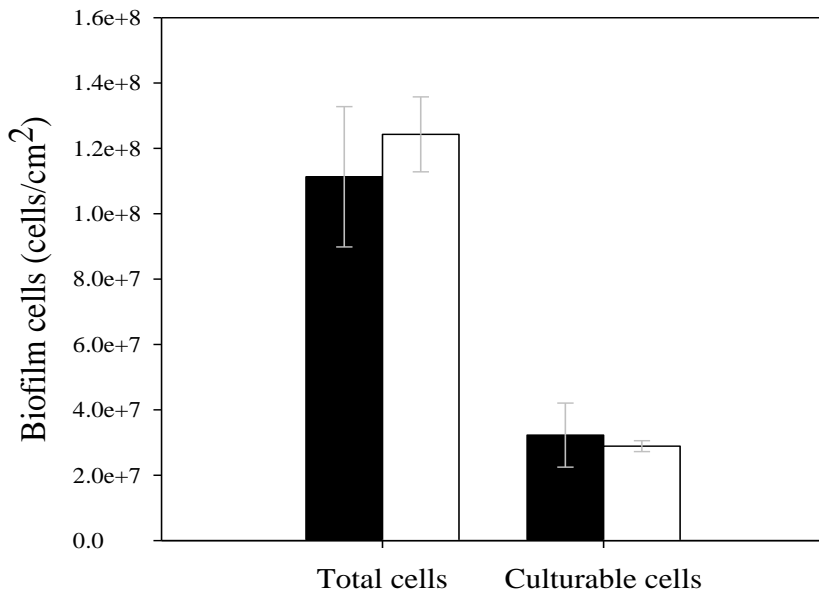


Figure 3. Number of total and culturable *E. coli* cells on PDMS after 24 h of biofilm formation at a flow rate of 2 mL/s (■; mimicking urinary catheters) and 4 mL/s (□; mimicking ureteral stents). The means \pm SDs for three independent experiments for each condition are presented.

The analysis of the biofilm cell number was complemented by their observation (Figure 4) and quantification (Figure 5) by confocal laser scanning microscopy (CLSM).

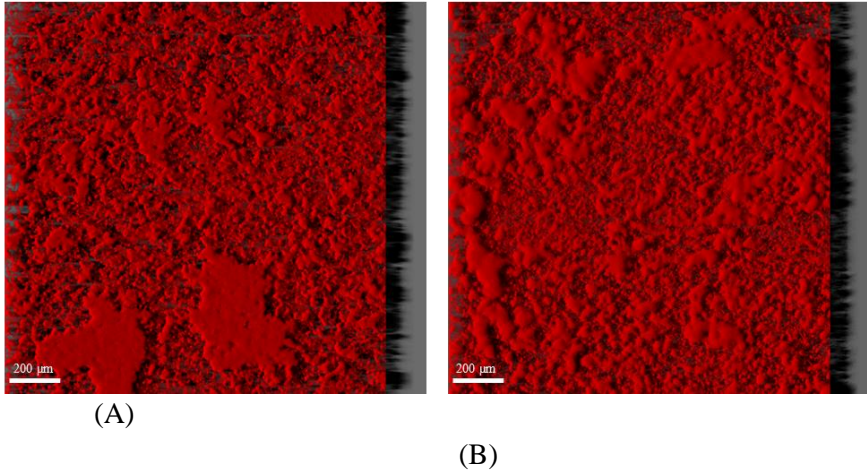


Figure 4. 3D projections of 24-h *E. coli* biofilms formed on PDMS at a flow rate of 2 mL/s (A; mimicking urinary catheters) and 4 mL/s (B; mimicking ureteral stents). These representative images were obtained from confocal z stacks using IMARIS software and present an aerial view of biofilm structures, with the shadow projection on the right. White bars correspond to 200 μm .

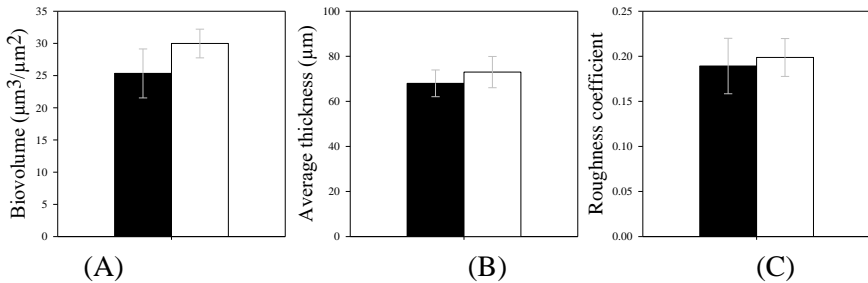


Figure 5. Biovolume (A), average thickness (B) and roughness coefficient (C) of 24-h *E. coli* biofilms formed on PDMS at a flow rate of 2 mL/s (■; mimicking urinary catheters) and 4 mL/s (□; mimicking ureteral stents). These quantitative parameters were obtained from confocal image series using the COMSTAT2 tool associated with the ImageJ software. The means \pm SDs for three independent experiments for each condition are presented.

This microscopic technique is a valuable tool for the study of biofilms developed on different surface materials, including those used in medical devices [133], as it allows the 3D visualization of fully hydrated, living specimens. In this work, the 24-h biofilms formed on PDMS surfaces placed inside the flow chamber were counterstained with Syto61

(Invitrogen, USA), a cell-permeant fluorescent nucleic acid stain, and observed using a Leica TCS SP5 II CLSM (Leica Microsystems, Germany). Three-dimensional projections of biofilm structures were reconstructed using the “Easy 3D” tool of IMARIS 8.4.1 software (Bitplane, Switzerland) directly from the *xyz* images series. Figure 4 presents representative CLSM images of biofilms developed on PDMS when exposed to a flow rate of 2 (Figure 4A) and 4 mL/s (Figure 4B). The two images are clearly similar, with thick biofilms with a dense and smooth appearance obtained at both flow rates.

Regarding quantification of biofilm structures, the COMSTAT2 tool associated with the ImageJ software was used to measure the biovolume ($\mu\text{m}^3/\mu\text{m}^2$), the average biofilm thickness (μm) and the roughness coefficient (Figure 5). Briefly, the biovolume is the overall volume occupied by the biofilm and an estimate of the biomass in the biofilm [134]. The average biofilm thickness provides a measure of the spatial size of the biofilm, while the roughness coefficient is a measure of variation in biofilm thickness across the field of view, giving an indication of biofilm heterogeneity [134].

The biovolume, thickness and roughness of the biofilm were maintained with increasing flow rate ($P > 0.05$, Figure 5), which reinforced the visual inspection of the biofilm structures (Figure 4).

When comparing all parameters obtained for the biofilm formed under two distinct hydrodynamic conditions (one that mimicked urine flow within urinary catheters and another that simulated fluid in ureteral stents), they were consistent with each other and follow the trend dictated by the adhesion results. Therefore, this study performed with the PPFC system suggests that the profile of initial adhesion can be used to estimate biofilm growth in urinary tract medical devices such as urinary catheters and ureteral stents.

CONCLUSION

PDMS has been widely used in the manufacture of urinary catheters and ureteral stents due to its outstanding properties. However, serious

complications are still arising due to biofilm formation on the surface of these indwelling devices. In the last years, numerous studies have been conducted in order to improve the antimicrobial and antifouling properties of PDMS-based surfaces. According to collected data, different strategies including the release of antimicrobial agents, contact-killing and anti-adhesive coatings, and surfaces that cause disruption of biofilm architecture by matrix degradation or quorum sensing interruption, have been proposed to prevent or delay biofilm formation on PDMS surfaces.

Despite the multiplicity of antibiofilm coatings for PDMS-based urinary devices, there is a need to develop new effective strategies, particularly for ureteral stents, where research in antibiofilm coatings is far less developed.

Flow cells are attractive *in vitro* platforms to evaluate biofilm growth on potential antimicrobial and antifouling surfaces under dynamic conditions. The experimental approach explored in this chapter showed the importance of using PPFCs in the investigation of cell adhesion and biofilm formation. Additionally, the PPFC results revealed that initial bacterial adhesion can be used to estimate biofilm growth in urinary tract devices such as urinary catheters and ureteral stents.

ACKNOWLEDGMENTS

This work was financially supported by: Base Funding - UIDB/00511/2020 of the Laboratory for Process Engineering, Environment, Biotechnology and Energy – LEPABE - funded by national funds through the FCT/MCTES (PIDDAC); and by project POCI-01-0145-FEDER-029589 funded by FEDER funds through COMPETE2020 – Programa Operacional Competitividade e Internacionalização (POCI) and by national funds (PIDDAC) through FCT/MCTES. R. Teixeira-Santos acknowledges the receipt of a Junior Researcher fellowship from this project. L. C. Gomes acknowledges the Junior Researcher contract (CEECIND/01700/2017) funded by national funds through FCT, I. P.

Support from the EU COST Actions ENBA (CA15216) and ENIUS (CA16217) is acknowledged.

REFERENCES

- [1] Kim, J. H., Park, H., and Seo, S. W. 2017. "In situ synthesis of silver nanoparticles on the surface of PDMS with high antibacterial activity and biosafety toward an implantable medical device." *Nano converg* 4:33.
- [2] Curtis, J. and Colas, A. 2013. "Chapter II.5.18 - Medical Applications of Silicones." In *Biomaterials Science (Third Edition)*, edited by B.D. Ratner, et al., 1106-1116. Academic Press.
- [3] Kendrick, T. C., Parbhoo, B. M., and White, J. W. 1989. "25 - Polymerization of Cyclosiloxanes." In *Comprehensive Polymer Science and Supplements*, edited by G. Allen and J.C. Bevington, 459-523. Amsterdam: Pergamon.
- [4] Shen, Q., Shan, Y., Lü, Y., Xue, P. et al. 2019. "Enhanced Antibacterial Activity of Poly (dimethylsiloxane) Membranes by Incorporating SiO₂ Microspheres Generated Silver Nanoparticles." *Nanomaterials (Basel, Switzerland)* 9:705.
- [5] Bhattacharjee, N., Urrios, A., Kang, S., and Folch, A. 2016. "The upcoming 3D-printing revolution in microfluidics." *Lab on a chip* 16:1720-1742.
- [6] ter Meulen, P. H., Berghmans, L. C. M., and van Kerrebroeck, P. E. V. A. 2003. "Systematic Review: Efficacy of Silicone Microimplants (Macroplastique®) Therapy for Stress Urinary Incontinence in Adult Women." *Eur Urol* 44:573-582.
- [7] Keskin, D., Mokabbar, T., Pei, Y., and Van Rijn, P. 2018. "The Relationship between Bulk Silicone and Benzophenone-Initiated Hydrogel Coating Properties." *Polymers (Basel)* 10:534.
- [8] Zhu, Z., Wang, Z., Li, S., and Yuan, X. 2019. "Antimicrobial strategies for urinary catheters." *J Biomed Mater Res A* 107:445-467.

- [9] Singha, P., Locklin, J., and Handa, H. 2017. "A review of the recent advances in antimicrobial coatings for urinary catheters." *Acta Biomater* 50:20-40.
- [10] Todd, A. M. and Knudsen, B. E. 2017. "Ureteral Stent Materials." In *Ureteric Stenting*, edited by R. Kulkarni, 83-90. Wiley.
- [11] Lawrence, E. L. and Turner, I. G. 2005. "Materials for urinary catheters: a review of their history and development in the UK." *Med Eng Phys* 27:443-453.
- [12] Liatsikos, E., Kallidonis, P., Stolzenburg, J. U., and Karnabatidis, D. 2009. "Ureteral stents: past, present and future." *Expert Rev Med Devices* 6:313-324.
- [13] Moola, S. and Konno, R. 2010. "A systematic review of the management of short-term indwelling urethral catheters to prevent urinary tract infections." *JBI Libr Syst Rev* 8:695-729.
- [14] Stenzelius, K., Persson, S., Olsson, U. B., and Stjarneblad, M. 2011. "Noble metal alloy-coated latex versus silicone Foley catheter in short-term catheterization: a randomized controlled study." *Scand J Urol Nephrol* 45:258-264.
- [15] Thibon, P., Le Coutour, X., Leroyer, R., and Fabry, J. 2000. "Randomized multi-centre trial of the effects of a catheter coated with hydrogel and silver salts on the incidence of hospital-acquired urinary tract infections." *J Hosp Infect* 45:117-124.
- [16] Hoe, J. W. 1989. "Antegrade double J ureteral stenting for ureteric strictures: use of silicone stents." *Australas Radiol* 33:385-389.
- [17] Tunney, M. M., Keane, P. F., Jones, D. S., and Gorman, S. P. 1996. "Comparative assessment of ureteral stent biomaterial encrustation." *Biomaterials* 17:1541-1546.
- [18] Weinstein, M. P., Towns, M. L., Quartey, S. M., Mirrett, S. et al. 1997. "The clinical significance of positive blood cultures in the 1990s: a prospective comprehensive evaluation of the microbiology, epidemiology, and outcome of bacteremia and fungemia in adults." *Clin Infect Dis* 24:584-602.
- [19] 2008. *Annual Epidemiological Report on Communicable Diseases in Europe 2008*. European Centre for Disease Prevention and Control.

- [20] Klevens, R. M., Edwards, J. R., Richards, C. L., Horan, T. C. et al. 2007. "Estimating health care-associated infections and deaths in U.S. hospitals, 2002." *Public Health Reports (Washington, D.C.:1974)* 122:160-166.
- [21] Alves, D., Vaz, A. T., Grainha, T., Rodrigues, C. F. et al. 2019. "Design of an Antifungal Surface Embedding Liposomal Amphotericin B Through a Mussel Adhesive-Inspired Coating Strategy." *Front Chem* 7:431.
- [22] Darouiche, Rabih O. 2001. "Device-Associated Infections: A Macroproblem that Starts with Microadherence." *Clin Infect Dis* 33:1567-1572.
- [23] Zarb, P., Coignard, B., Griskeviciene, J., Muller, A. et al. 2012. "The European Centre for Disease Prevention and Control (ECDC) pilot point prevalence survey of healthcare-associated infections and antimicrobial use." *Euro surveillance : bulletin Europeen sur les maladies transmissibles = European communicable disease bulletin* 17:20316.
- [24] Magill, S. S., Edwards, J. R., Bamberg, W., Beldavs, Z. G. et al. 2014. "Multistate point-prevalence survey of health care-associated infections." *N Engl J Med* 370:1198-1208.
- [25] Donlan, R. M. 2001. "Biofilms and device-associated infections." *Emerg Infect Dis* 7:277-281.
- [26] Mulhall, A. B., Chapman, R. G., and Crow, R. A. 1988. "Bacteriuria during indwelling urethral catheterization." *J Hosp Infect* 11:253-262.
- [27] Richter, S., Ringel, A., Shalev, M., and Nissenkorn, I. 2000. "The indwelling ureteric stent: a 'friendly' procedure with unfriendly high morbidity." *BJU International* 85:408-411.
- [28] Nicolle, L. E. 2005. "Complicated urinary tract infection in adults." *Can J Infect Dis Med Microbiol* 16:349-360.
- [29] Riedl, C. R., Plas, E., Hübner, W. A., Zimmerl, H. et al. 1999. "Bacterial colonization of ureteral stents." *Eur Urol* 36:53-59.

- [30] Foxman, B. 2002. "Epidemiology of urinary tract infections: incidence, morbidity, and economic costs." *Am J Med* 113 Suppl:5S-13S.
- [31] Scott II, R. D. 2009. *The direct medical costs of healthcare-associated infections in the US hospitals and the benefits of prevention.*
- [32] Feneley, R., Hopley, I., and Wells, P. 2015. "Urinary catheters: history, current status, adverse events and research agenda." *J Med Eng Technol* 39:459-470.
- [33] Staubli, S. E. L., Mordasini, L., Engeler, D. S., Sauter, R. et al. 2016. "Economic Aspects of Morbidity Caused by Ureteral Stents." *Urol Int* 97:91-97.
- [34] Maki, D. G. and Tambyah, P. A. 2001. "Engineering out the risk for infection with urinary catheters." *Emerg Infect Dis* 7:342-347.
- [35] Jacobsen, S. M., Stickler, D. J., Mobley, H. L. T., and Shirliff, M. E. 2008. "Complicated catheter-associated urinary tract infections due to *Escherichia coli* and *Proteus mirabilis*." *Clin Microbiol Rev* 21:26-59.
- [36] Costerton, J. W., Stewart, P. S., and Greenberg, E. P. 1999. "Bacterial biofilms: a common cause of persistent infections." *Science* (New York, N.Y.) 284:1318-1322.
- [37] Flemming, H.-C. and Wingender, J. 2010. "The biofilm matrix." *Nat Rev Microbiol* 8:623-633.
- [38] Garrett, T. R., Bhakoo, M., and Zhang, Z. 2008. "Bacterial adhesion and biofilms on surfaces." *Prog Nat Sci* 18:1049-1056.
- [39] Briandet, R., Herry, J.-M., and Bellon-Fontaine, M.-N. 2001. "Determination of the van der Waals, electron donor and electron acceptor surface tension components of static Gram-positive microbial biofilms." *Colloids Surf B Biointerfaces* 21:299-310.
- [40] Katsikogianni, M. and Missirlis, Y. 2004. "Concise review of mechanisms of bacterial adhesion to biomaterials and of techniques used in estimating bacteria-material interactions." *Eur Cells Mater* 8:37-57.

- [41] De Weger, L. A., van der Vlugt, C. I., Wijffjes, A. H., Bakker, P. A. et al. 1987. "Flagella of a plant-growth-stimulating *Pseudomonas fluorescens* strain are required for colonization of potato roots." *J Bacteriol* 169:2769-2773.
- [42] Ganderton, L., Chawla, J., Winters, C., Wimpenny, J. et al. 1992. "Scanning electron microscopy of bacterial biofilms on indwelling bladder catheters." *Eur J Clin Microbiol Infect Dis* 11:789-796.
- [43] Stewart, P. S. and Costerton, J. W. 2001. "Antibiotic resistance of bacteria in biofilms." *Lancet* (London, England) 358:135-138.
- [44] Lewis, K. 2007. "Persister cells, dormancy and infectious disease." *Nat Rev Microbiol* 5:48-56.
- [45] Morris, N. S. and Stickler, D. J. 1998. "Encrustation of indwelling urethral catheters by *Proteus mirabilis* biofilms growing in human urine." *J Hosp Infect* 39:227-234.
- [46] Broomfield, R. J., Morgan, S. D., Khan, A., and Stickler, D. J. 2009. "Crystalline bacterial biofilm formation on urinary catheters by urease-producing urinary tract pathogens: a simple method of control." *J Med. Microbiol* 58:1367-1375.
- [47] Tenke, P., Köves, B., Nagy, K., Hultgren, S. J. et al. 2012. "Update on biofilm infections in the urinary tract." *World J Urol* 30:51-57.
- [48] Dakal, T. C., Kumar, A., Majumdar, R. S., and Yadav, V. 2016. "Mechanistic Basis of Antimicrobial Actions of Silver Nanoparticles." *Front Microbiol* 7:1831.
- [49] Ahearn, D. G., Grace, D. T., Jennings, M. J., Borazjani, R. N. et al. 2000. "Effects of hydrogel/silver coatings on in vitro adhesion to catheters of bacteria associated with urinary tract infections." *Curr Microbiol* 41:120-125.
- [50] Ogilvie, A. T., Brisson, B. A., Singh, A., and Weese, J. S. 2015. "In vitro evaluation of the impact of silver coating on *Escherichia coli* adherence to urinary catheters." *Can Vet J* 56:490-494.
- [51] Cooper, I. R., Pollini, M., and Paladini, F. 2016. "The potential of photo-deposited silver coatings on Foley catheters to prevent urinary tract infections." *Mater Sci Eng C* 69:414-420.

- [52] Dayyoub, E., Frant, M., Pinnapireddy, S. R., Liefeyth, K. et al. 2017. "Antibacterial and anti-encrustation biodegradable polymer coating for urinary catheter." *Int J Pharm* 531:205-214.
- [53] Heidari Zare, H., Juhart, V., Vass, A., Franz, G. et al. 2017. "Efficacy of silver/hydrophilic poly(p-xylylene) on preventing bacterial growth and biofilm formation in urinary catheters." *Biointerphases* 12:011001.
- [54] Zhang, S., Wang, L., Liang, X., Vorstius, J. et al. 2019. "Enhanced Antibacterial and Antiadhesive Activities of Silver-PTFE Nanocomposite Coating for Urinary Catheters." *ACS Biomater Sci Eng* 5:2804-2814.
- [55] Wang, L., Zhang, S., Keatch, R., Corner, G. et al. 2019. "In-vitro antibacterial and anti-encrustation performance of silver-polytetrafluoroethylene nanocomposite coated urinary catheters." *J Hosp Infect* 103:55-63.
- [56] Simhi, E., van der Mei, H. C., Ron, E. Z., Rosenberg, E. et al. 2000. "Effect of the adhesive antibiotic TA on adhesion and initial growth of *E. coli* on silicone rubber." *FEMS Microbiol Lett* 192:97-100.
- [57] Chaiban, G., Hanna, H., Dvorak, T., and Raad, I. 2005. "A rapid method of impregnating endotracheal tubes and urinary catheters with gendine: a novel antiseptic agent." *J Antimicrob Chemoth* 55:51-56.
- [58] Belfield, K., Chen, X., Smith, E. F., Ashraf, W. et al. 2019. "An antimicrobial impregnated urinary catheter that reduces mineral encrustation and prevents colonisation by multi-drug resistant organisms for up to 12 weeks." *Acta Biomater* 90:157-168.
- [59] Kazmierska, K. A., Thompson, R., Morris, N., Long, A. et al. 2010. "In Vitro Multicompartmental Bladder Model for Assessing Blockage of Urinary Catheters: Effect of Hydrogel Coating on Dynamics of *Proteus mirabilis* Growth." *Urology* 76:515.e15-515.e20.
- [60] Gonçalves, I., Abreu, A. S., Matamá, T., Ribeiro, A. et al. 2015. "Enzymatic synthesis of poly(catechin)-antibiotic conjugates: an

- antimicrobial approach for indwelling catheters." *Appl Microbiol Biotechnol* 99:637-651.
- [61] Adlhart, C., Verran, J., Azevedo, N. F., Olmez, H. et al. 2018. "Surface modifications for antimicrobial effects in the healthcare setting: a critical overview." *J Hosp Infect* 99:239-249.
- [62] Li, X., Li, P., Saravanan, R., Basu, A. et al. 2014. "Antimicrobial functionalization of silicone surfaces with engineered short peptides having broad spectrum antimicrobial and salt-resistant properties." *Acta Biomater* 10:258-266.
- [63] Raman, N., Lee, M.-R., Rodríguez López, A. d. L., Palecek, S. P. et al. 2016. "Antifungal activity of a β -peptide in synthetic urine media: Toward materials-based approaches to reducing catheter-associated urinary tract fungal infections." *Acta Biomater* 43:240-250.
- [64] Lim, K., Chua, R. R. Y., Ho, B., Tambyah, P. A. et al. 2015. "Development of a catheter functionalized by a polydopamine peptide coating with antimicrobial and antibiofilm properties." *Acta Biomater* 15:127-138.
- [65] Lim, K., Saravanan, R., Chong, K. K. L., Goh, S. H. M. et al. 2018. "Anhydrous polymer-based coating with sustainable controlled release functionality for facile, efficacious impregnation, and delivery of antimicrobial peptides." *Biotechnol Bioeng* 115:2000-2012.
- [66] Xu, L. C. and Siedlecki, C. A. 2017. "Protein adsorption, platelet adhesion, and bacterial adhesion to polyethylene-glycol-textured polyurethane biomaterial surfaces." *J Biomed Mater Res B Appl Biomater* 105:668-678.
- [67] Cheng, G., Zhang, Z., Chen, S., Bryers, J. D. et al. 2007. "Inhibition of bacterial adhesion and biofilm formation on zwitterionic surfaces." *Biomaterials* 28:4192-4199.
- [68] Park, J. H., Lee, K. B., Kwon, I. C., and Bae, Y. H. 2001. "PDMS-based polyurethanes with MPEG grafts: mechanical properties, bacterial repellency, and release behavior of rifampicin." *J Biomater Sci Polym Ed* 12:629-645.

- [69] Park, J. H., Cho, Y. W., Kwon, I. C., Jeong, S. Y. et al. 2002. "Assessment of PEO/PTMO multiblock copolymer/segmented polyurethane blends as coating materials for urinary catheters: in vitro bacterial adhesion and encrustation behavior." *Biomaterials* 23:3991-4000.
- [70] Yong, Y., Qiao, M., Chiu, A., Fuchs, S. et al. 2019. "Conformal Hydrogel Coatings on Catheters To Reduce Biofouling." *Langmuir* 35:1927-1934.
- [71] Chung, P. H., Wong, C. W., Lai, C. K., Siu, H. K. et al. 2017. "A prospective interventional study to examine the effect of a silver alloy and hydrogel-coated catheter on the incidence of catheter-associated urinary tract infection." *Hong Kong Med J* 23:239-245.
- [72] Diaz Blanco, C., Ortner, A., Dimitrov, R., Navarro, A. et al. 2014. "Building an Antifouling Zwitterionic Coating on Urinary Catheters Using an Enzymatically Triggered Bottom-Up Approach." *ACS Appl Mater Interfaces* 6:11385-11393.
- [73] Vaterrodt, A., Thallinger, B., Daumann, K., Koch, D. et al. 2016. "Antifouling and Antibacterial Multifunctional Polyzwitterion/Enzyme Coating on Silicone Catheter Material Prepared by Electrostatic Layer-by-Layer Assembly." *Langmuir* 32:1347-1359.
- [74] Fan, Y.-J., Pham, M. T., and Huang, C.-J. 2019. "Development of Antimicrobial and Antifouling Universal Coating via Rapid Deposition of Polydopamine and Zwitterionization." *Langmuir* 35:1642-1651.
- [75] Tyler, B. J., Hook, A., Pelster, A., Williams, P. et al. 2017. "Development and characterization of a stable adhesive bond between a poly(dimethylsiloxane) catheter material and a bacterial biofilm resistant acrylate polymer coating." *Biointerphases* 12:02C412.
- [76] Burton, E., Gawande, P. V., Yakandawala, N., LoVetri, K. et al. 2006. "Antibiofilm activity of GlmU enzyme inhibitors against catheter-associated uropathogens." *Antimicrob Agents Chemother* 50:1835-1840.

- [77] Thompson, V. C., Adamson, P. J., Dilag, J., Uswatte Uswatte Liyanage, D. B. et al. 2016. "Biocompatible anti-microbial coatings for urinary catheters." *RSC Adv* 6:53303-53309.
- [78] Adlington, K., Nguyen, N. T., Eaves, E., Yang, J. et al. 2016. "Application of Targeted Molecular and Material Property Optimization to Bacterial Attachment-Resistant (Meth)acrylate Polymers." *Biomacromolecules* 17:2830-2838.
- [79] Zhou, C., Wu, Y., Thappeta, K. R. V., Subramanian, J. T. L. et al. 2017. "In Vivo Anti-Biofilm and Anti-Bacterial Non-Leachable Coating Thermally Polymerized on Cylindrical Catheter." *ACS Appl Mater Interfaces* 9:36269-36280.
- [80] Keum, H., Kim, J. Y., Yu, B., Yu, S. J. et al. 2017. "Prevention of Bacterial Colonization on Catheters by a One-Step Coating Process Involving an Antibiofouling Polymer in Water." *ACS Appl Mater Interfaces* 9:19736-19745.
- [81] Guildford, A., Morris, C., Kitt, O., and Cooper, I. 2018. "The effect of urinary Foley catheter substrate material on the antimicrobial potential of calixerene-based molecules." *J Appl Microbiol* 124:1047-1059.
- [82] Ivanova, K., Fernandes, M. M., Francesko, A., Mendoza, E. et al. 2015. "Quorum-Quenching and Matrix-Degrading Enzymes in Multilayer Coatings Synergistically Prevent Bacterial Biofilm Formation on Urinary Catheters." *ACS Appl Mater Interfaces* 7:27066-27077.
- [83] Ivanova, K., Fernandes, M. M., Mendoza, E., and Tzanov, T. 2015. "Enzyme multilayer coatings inhibit *Pseudomonas aeruginosa* biofilm formation on urinary catheters." *Appl Microbiol Biotechnol* 99:4373-4385.
- [84] Cormio, L., LaForgia, P., LaForgia, D., Siitonen, A. et al. 1997. "Is it possible to prevent bacterial adhesion onto ureteric stents?" *Urol Res* 25:213-216.
- [85] Frant, M., Dayyoub, E., Bakowsky, U., and Liefieith, K. 2018. "Evaluation of a ureteral catheter coating by means of a BioEncrustation in vitro model." *Int J Pharm* 546:86-96.

- [86] Ko, R., Cadieux, P. A., Dalsin, J. L., Lee, B. P. et al. 2008. "First prize: Novel uropathogen-resistant coatings inspired by marine mussels." *J Endourol* 22:1153-1160.
- [87] Stickler, D. J., Evans, A., Morris, N., and Hughes, G. 2002. "Strategies for the control of catheter encrustation." *Int J Antimicrob Agents* 19:499-506.
- [88] Graham, V. M. and Cady, C. N. 2014. "Nano and Microscale Topographies for the Prevention of Bacterial Surface Fouling." *Coatings* 4:37-59.
- [89] Wen, G., Guo, Z., and Liu, W. 2017. "Biomimetic polymeric superhydrophobic surfaces and nanostructures: from fabrication to applications." *Nanoscale* 9:3338-3366.
- [90] Bixler, G. D., Theiss, A., Bhushan, B., and Lee, S. C. 2014. "Anti-fouling properties of microstructured surfaces bio-inspired by rice leaves and butterfly wings." *J Colloid Interface Sci* 419:114-133.
- [91] Pereira, M. O., Kuehn, M., Wuertz, S., Neu, T. et al. 2002. "Effect of flow regime on the architecture of a *Pseudomonas fluorescens* biofilm." *Biotechnol Bioeng* 78:164-171.
- [92] Moreira, J. M. R., Araújo, J. D., Miranda, J. M., Simões, M. et al. 2014. "The effects of surface properties on *Escherichia coli* adhesion are modulated by shear stress." *Colloids Surf B Biointerfaces* 123:1-7.
- [93] Millsap, K. W., Reid, G., van der Mei, H. C., and Busscher, H. J. 1997. "Adhesion of *Lactobacillus* species in urine and phosphate buffer to silicone rubber and glass under flow." *Biomaterials* 18:87-91.
- [94] McClaine, J. W. and Ford, R. M. 2002. "Characterizing the adhesion of motile and nonmotile *Escherichia coli* to a glass surface using a parallel-plate flow chamber." *Biotechnol Bioeng* 78:179-189.
- [95] Ammons, M. C. B., Ward, L. S., and James, G. A. 2011. "Anti-biofilm efficacy of a lactoferrin/xylitol wound hydrogel used in combination with silver wound dressings." *Int Wound J* 8:268-273.

- [96] Carlson, R. P., Taffs, R., Davison, W. M., and Stewart, P. S. 2008. "Anti-biofilm properties of chitosan-coated surfaces." *J Biomater Sci Polym Ed* 19:1035-1046.
- [97] Goeres, D. M., Hamilton, M. A., Beck, N. A., Buckingham-Meyer, K. et al. 2009. "A method for growing a biofilm under low shear at the air-liquid interface using the drip flow biofilm reactor." *Nat Protoc* 4:783-788.
- [98] Azeredo, J., Azevedo, N. F., Briandet, R., Cerca, N. et al. 2017. "Critical review on biofilm methods." *Crit Rev Microbiol* 43:313-351.
- [99] Lawrence, J. R., Swerhone, G. D., and Neu, T. R. 2000. "A simple rotating annular reactor for replicated biofilm studies." *J Microbiol Methods* 42:215-224.
- [100] Coenye, T. and Nelis, H. J. 2010. "In vitro and in vivo model systems to study microbial biofilm formation." *J Microbiol Methods* 83:89-105.
- [101] Willcock, L., Gilbert, P., Holah, J., Wirtanen, G. et al. 2000. "A new technique for the performance evaluation of clean-in-place disinfection of biofilms." *J Ind Microbiol Biotechnol* 25:235-241.
- [102] Lee, J. H., Kaplan, J. B., and Lee, W. Y. 2008. "Microfluidic devices for studying growth and detachment of *Staphylococcus epidermidis* biofilms." *Biomed Microdevices* 10:489-498.
- [103] Tremblay, Y. D., Vogeleer, P., Jacques, M., and Harel, J. 2015. "High-throughput microfluidic method to study biofilm formation and host-pathogen interactions in pathogenic *Escherichia coli*." *Appl Environ Microbiol* 81:2827-2840.
- [104] Shields, R. C. and Burne, R. A. 2016. "Growth of *Streptococcus mutans* in Biofilms Alters Peptide Signaling at the Sub-population Level." *Front Microbiol* 7:1075.
- [105] Situma, C., Hashimoto, M., and Soper, S. A. 2006. "Merging microfluidics with microarray-based bioassays." *Biomol Eng* 23:213-231.

- [106] Wessel, A. K., Hmelo, L., Parsek, M. R., and Whiteley, M. 2013. "Going local: technologies for exploring bacterial micro-environments." *Nat Rev Microbiol* 11:337-348.
- [107] Abaci, H., Drazer, G., and Gerecht, S. 2013. "Recapitulating the vascular microenvironment in microfluidic platforms." *Nano LIFE* 03:1340001.
- [108] Nickel, J. C., Ruseska, I., Wright, J. B., and Costerton, J. W. 1985. "Tobramycin resistance of *Pseudomonas aeruginosa* cells growing as a biofilm on urinary catheter material." *Antimicrob Agents Chemother* 27:619-624.
- [109] Azevedo, A. S., Almeida, C., Gomes, L. C., Ferreira, C. et al. 2017. "An in vitro model of catheter-associated urinary tract infections to investigate the role of uncommon bacteria on the *Escherichia coli* microbial consortium." *Biochem Eng J* 118:64-69.
- [110] Salanitro, J. and Hokanson, J. 1990. "Tubular Biofilm Reactor."
- [111] McCoy, W. F., Bryers, J. D., Robbins, J., and Costerton, J. W. 1981. "Observations of fouling biofilm formation." *Can J Microbiol* 27:910-917.
- [112] Linton, C. J., Sherriff, A., and Millar, M. R. 1999. "Use of a modified Robbins device to directly compare the adhesion of *Staphylococcus epidermidis* RP62A to surfaces." *J Appl Microbiol* 86:194-202.
- [113] Teodósio, J. S., Silva, F. C., Moreira, J. M. R., Simões, M. et al. 2013. "Flow cells as quasi-ideal systems for biofouling simulation of industrial piping systems." *Biofouling* 29:953-966.
- [114] Simões, M., Pereira, M. O., Sillankorva, S., Azeredo, J. et al. 2007. "The effect of hydrodynamic conditions on the phenotype of *Pseudomonas fluorescens* biofilms." *Biofouling* 23:249-258.
- [115] Teodósio, J. S., Simões, M., Melo, L. F., and Mergulhão, F. J. 2011. "Flow cell hydrodynamics and their effects on *E. coli* biofilm formation under different nutrient conditions and turbulent flow." *Biofouling* 27:1-11.

- [116] Teodósio, J. S., Simões, M., and Mergulhão, F. J. 2012. "The influence of nonconjugative *Escherichia coli* plasmids on biofilm formation and resistance." *J Appl Microbiol* 113:373-382.
- [117] Teodósio, J. S., Simões, M., Alves, M. A., Melo, L. F. et al. 2012. "Setup and validation of flow cell systems for biofouling simulation in industrial settings." *Sci World J* 2012:10.
- [118] Chin, M. Y. H., Busscher, H. J., Evans, R., Noar, J. et al. 2006. "Early biofilm formation and the effects of antimicrobial agents on orthodontic bonding materials in a parallel plate flow chamber." *Eur J Orthod* 28:1-7.
- [119] van der Borden, A. J., van der Werf, H., van der Mei, H. C., and Busscher, H. J. 2004. "Electric current-induced detachment of *Staphylococcus epidermidis* biofilms from surgical stainless steel." *Appl Environ Microbiol* 70:6871-6874.
- [120] Lopez-Mila, B., Alves, P., Riedel, T., Dittrich, B. et al. 2018. "Effect of shear stress on the reduction of bacterial adhesion to antifouling polymers." *Bioinspir Biomim* 13:065001.
- [121] Alves, P., Nir, S., Reches, M., and Mergulhão, F. 2018. "The effects of fluid composition and shear conditions on bacterial adhesion to an antifouling peptide-coated surface." *MRS Commun* 8:938-946.
- [122] Velraeds, M. M., van de Belt-Gritter, B., van der Mei, H. C., Reid, G. et al. 1998. "Interference in initial adhesion of uropathogenic bacteria and yeasts to silicone rubber by a *Lactobacillus acidophilus* biosurfactant." *J Med Microbiol* 47:1081-1085.
- [123] Mosayyebi, A., Yue, Q. Y., Somani, B. K., Zhang, X. et al. 2018. "Particle accumulation in ureteral stents is governed by fluid dynamics: in vitro study using a "stent-on-chip" model." *J Endourol* 32:639-646.
- [124] Van Oss, C. J., Chaudhury, M. K., and Good, R. J. 1987. "Monopolar surfaces." *Adv Colloid Interface Sci* 28:35-64.
- [125] Van Oss, C. J., Good, R. J., and Chaudhury, M. K. 1988. "Additive and nonadditive surface tension components and the interpretation of contact angles." *Langmuir* 4:884-891.

- [126] Van Oss, C. J., Ju, L., Chaudhury, M. K., and Good, R. J. 1989. "Estimation of the polar parameters of the surface tension of liquids by contact angle measurements on gels." *J Colloid Interface Sci* 128:313-319.
- [127] Aryal, B. and Neuner, G. 2009. "Leaf wettability decreases along an extreme altitudinal gradient." *Oecologia* 162:1.
- [128] Sjollema, J., Busscher, H. J., and Weerkamp, A. H. 1988. "Deposition of oral streptococci and polystyrene latices onto glass in a parallel plate flow cell." *Biofouling* 1:101-112.
- [129] Bakker, D. P., van der Plaats, A., Verkerke, G. J., Busscher, H. J. et al. 2003. "Comparison of velocity profiles for different flow chamber designs used in studies of microbial adhesion to surfaces." *Appl Environ Microbiol* 69:6280-6287.
- [130] Koseoglu, H., Aslan, G., Esen, N., Sen, B. H. et al. 2006. "Ultrastructural stages of biofilm development of *Escherichia coli* on urethral catheters and effects of antibiotics on biofilm formation." *Urology* 68:942-946.
- [131] Barbosa, J., Cuppini, M., Flach, J., Steffens, C. et al. 2016. "Removal of *Escherichia coli* in boning knives with different sanitizers." *LWT - Food Sci Technol* 71:309-315.
- [132] Gomes, L. C., Silva, L. N., Simoes, M., Melo, L. F. et al. 2015. "*Escherichia coli* adhesion, biofilm development and antibiotic susceptibility on biomedical materials." *J Biomed Mater Res A* 103:1414-1423.
- [133] Adair, C. G., Gorman, S. P., Byers, L. B., Jones, D. S. et al. 2000. "Confocal Laser Scanning Microscopy for Examination of Microbial Biofilms." In *Handbook of Bacterial Adhesion: Principles, Methods, and Applications*, edited by Y.H. An and R.J. Friedman, 249-257. Totowa, NJ: Humana Press.
- [134] Heydorn, A., Nielsen, A. T., Hentzer, M., Sternberg, C. et al. 2000. "Quantification of biofilm structures by the novel computer program COMSTAT." *Microbiology* 146 (Pt 10):2395-2407.